Effects of Microstate Dynamic Brain Network Disruption in Different Stages of Schizophrenia

Tianyi Yan, *Member, IEEE*, Gongshu Wang, Tiantian Liu, Guoqi Li, *Member, IEEE*, Changming Wang, Shintaro Funahashi, Dingjie Suo, and Guangying Pei

***Abstract*— Schizophrenia is a heterogeneous mental disorder with unknown etiology or pathological characteristics. Microstate analysis of the electroencephalogram (EEG) signal has shown significant potential value for clinical research. Importantly, significant changes in microstate-specific parameters have been extensively reported; however, these studies have ignored the information interactions within the microstate network in different stages of schizophrenia. Based on recent findings, since rich information about the functional organization of the brain can be revealed by functional connectivity dynamics, we use the first-order autoregressive model to construct the functional connectivity of intra- and intermicrostate networks to identify information interactions among microstate networks. We demonstrate that, beyond abnormal parameters, disrupted organization of the microstate networks plays a crucial role in different stages of the disease by 128-channel EEG data collected from individuals with first-episode schizophrenia, ultrahigh-risk, familial high-risk, and healthy controls. According to the characteristics of the microstates of patients at different stages, the parameters of microstate class A are reduced, those of class C are increased, and the transitions from intra- to intermicrostate functional connectivity are gradually disrupted. Furthermore, decreased integration of intermicrostate information might lead to cognitive deficits in individuals with schizophrenia and those in high-risk states. Taken together, these findings illustrate that the dynamic functional connectivity of intra- and intermicrostate networks captures more components of disease pathophysiology. Our work sheds new light on the characterization of dynamic functional brain networks based on EEG signals and provides a new interpretation of aberrant brain function in different stages of schizophrenia from the perspective of microstates.**

***Index Terms*— Dynamic brain network, information interaction, microstates, resting-state EEG, schizophrenia stages.**

I. Introduction

SCHIZOPHRENIA is a heterogeneous mental disorder with unknown etiology or pathological characteristics [1]. According to the description of the neurodevelopmental model, the trajectory of schizophrenia is divided into four stages. The first stage is defined as the high-risk (HR) stage before a detectable defect, such as being a first-degree relative of a person with schizophrenia. The second stage is called the ultrahigh-risk (UHR) stage and represents the period before the first-episode of schizophrenia (FES). Imaging studies have shown that brain networks in schizophrenia are aberrant and remain elusive [2].

As a promising method for studying the neurophysiology of the brain, electroencephalogram (EEG) microstates (MSs) can be used to classify and evaluate brain network dynamics in health and disease at millisecond-level timescales, and these techniques have gained increasing popularity in recent years [3], [4]. EEG MSs have provided enticing early results on their potential clinical value under certain conditions of schizophrenia [5]. In the past 15 years, a growing number of studies have reported significant differences in the spatiotemporal characteristics of EEG MS in patients with schizophrenia or psychosis compared with healthy controls [6], [7], [8], [9], [10], [11], [12]. The most commonly discussed in the literature is the increase in MS class C activity and the decrease in MS class D activity. However, the results of all studies are different, and the influence of the data processing method and selection of the control group cannot be ruled out. Two studies have mentioned that schizophrenia patients employ different concatenations of MSs [13], [14]. EEG MSs have also been identified as a potential biomarker for early diagnosis and predictive risk of schizophrenia [5], [15]. Nevertheless, less attention has been given to simultaneously assessing the impact of MSs in different stages of schizophrenia on clinical symptoms and cognitive function.

Manuscript received 14 October 2022; revised 12 February 2023 and 31 March 2023; accepted 26 May 2023. Date of publication 7 June 2023; date of current version 16 June 2023. This work was supported in part by the Scientific and Technological Innovation (STI) 2030—Major Projects under Grant 2022ZD0208500; in part by the National Natural Science Foundation of China under Grant U20A20191, Grant 82071912, Grant 12104049, and Grant 82202291; and in part by the Fundamental Research Funds for the Central Universities under Grant 2023CX01024. *(Corresponding authors: Guangying Pei; Dingjie Suo.)*

This work involved human subjects or animals in its research. Approval of all ethical and experimental procedures and protocols was granted by the Science and Ethics Committee of the Beijing Anding Hospital of Capital Medical University, and performed in line with the Declaration of Helsinki.

Tianyi Yan, Gongshu Wang, Tiantian Liu, Dingjie Suo, and Guangying Pei are with the School of Life Science, Beijing Institute of Technology, Beijing 100081, China (e-mail: yantianyi@bit.edu.cn; gongshu@bit.edu.cn; tiantian2bit@bit.edu.cn; suo@bit.edu.cn; pei_guangying@bit.edu.cn).

Guoqi Li is with the Institute of Automation, Chinese Academy of Sciences, Beijing 100080, China (e-mail: guoqi.li@ia.ac.cn).

Changming Wang is with the Department of Neurosurgery, XuanWu Hospital, Capital Medical University, Beijing 100088, China (e-mail: superwcm@gmail.com).

Shintaro Funahashi is with the Advanced Research Institute of Multidisciplinary Science, Beijing Institute of Technology, Beijing 100081, China (e-mail: funahashi@bit.edu.cn).

This article has supplementary downloadable material available at https://doi.org/10.1109/TNSRE.2023.3283708, provided by the authors.

Digital Object Identifier 10.1109/TNSRE.2023.3283708

In addition, since EEG MSs have been referred to as a conceptual analogy, they reflect the coordinated activity of neural ensembles in the brain [16]. A few recent studies have suggested that MS maps correlate with the activity of particular resting-state networks (RSNs) identified by functional magnetic resonance imaging (fMRI). In particular, MS classes A, B, C, and D are reported to correspond to RSNs recognized as phonological processing, visual network, salience network, and attention network, respectively, and may share the same neurophysiological substrates. MS time series may correspond to different functional connections (FCs) between RSNs [17]. The characteristics of EEG MSs can be used to quantify the operation of large-scale brain networks, and the transitions of different MS classes reflect the dynamics of brain activity states [18]. Resting-state EEG MSs are thought to reflect local instantaneous states and global interactions of distributed neural networks in the brain [12]. Furthermore, studies have shown that EEG MSs are better conceptualized as spatial and temporal continuity [19] and provide novel information about the architecture of brain connections not available with fMRI [20], [21]. Therefore, abnormal MSs in schizophrenia may indicate disruption of normal network activities that underlie disease pathogenesis. Recently, only a few studies have focused on the relationship between MSs and brain networks. Yao et al. constructed a brain functional network using 64 scalp electrodes and phase-locked values of MS time series to discriminate differences in working memory between schizophrenia patients and healthy controls while reducing time complexity [22]. A combination of MS analysis and entropy measures revealed abnormally chaotic transitions between brain networks in early-course psychosis patients [20].

However, despite these encouraging findings on the EEG functional network by EEG MS time series, the relationships between EEG MS connectivity networks and clinical characteristics of psychosis patients remain ambiguous. According to the "atoms of thought" hypothesis, MS syntax contains important information about underlying neural generators, and MSs are constantly changing even when the brain is resting [16]. The information interactions within the same types of MSs and between different types of MSs, which represent a special class of connection states arising from microscopic dynamics, can be assumed to implement the maintenance of and dynamic changes in brain states, respectively. Therefore, here, we introduce a novel approach to explore the intra- or intermicrostate FCs derived from the same or different types of MSs. Different from traditional FC studies that analyzed the comprehensive connectivity patterns in brain activity, the intra- and intermicrostate FCs reveal how the brain changes and maintains microstates, respectively, which are essential for the normal function of the brain. Importantly, we applied the method to explore the intra- and intermicrostate properties of FC across the FES, UHR, HR, and healthy control (HC) groups. These findings shed new light on the pathological mechanisms revealed in schizophrenia and high-risk states from the perspective of EEG MSs.

The major merits of this work are shown below:

1) We proposed a novel approach to explore brain networks based on intra- and intermicrostates; that is, we constructed dynamic FCs (dFCs) from the same or different types of MS time series, which were extracted from the original MS time series.
2) We discovered that the organization of dFCs of intra- and intermicrostate networks, characterized by topological metrics, is gradually disrupted with different disease stages.
3) We compared the brain networks constructed by traditional methods and those of MSs proposed by us and discovered that intra- and intermicrostate brain networks were closely related to patients' cognitive decline and disease status, which could better reflect underlying disease processes.

The remainder of this article is organized as follows. Section II introduces the conventional MS analysis method, which obtains the MS time series and calculates its spatiotemporal characteristics. Section III introduces our MS brain networks and provides analyses of topological metrics and interpretability of the disease state. Section IV verifies the effect of our methods on resting-state EEG datasets and clinical scores across different stages of schizophrenia and discovers that the MS brain networks reveal more disease information than traditional networks. Section V provides some further discussion about our experiments. Section VI concludes this work.

II. Preliminary Knowledge

Brain activity processes vary in the subsecond range, and EEG can be measured in milliseconds with satisfactory temporal resolution. Traditionally, the analysis of EEG data focuses more on the time domain, which reflects the high temporal resolution of EEG data while ignoring the information at the topological level. The instantaneous spatial configuration of the brain's electric field directly reflects the dynamic state of the brain. Since changes in the EEG configuration are discontinuous, while a given field configuration tends to remain quasistable for subsecond periods, it rapidly changes to a different configuration. These periods of quasisteady-state field configuration, known as MS, characterize fundamental steps in the brain's information processing [15], [23].

EEG MS analysis is able to simultaneously consider signals from all electrodes throughout the brain to create a global representation of functional state, while being suggested to reflect the resting-state spontaneous activity of the human brain and its event-related effects on stimulus processing. Furthermore, the observed MS configurations are concentrated in several classes of field configurations, which can be identified by spatial clustering [16], [24].

The EEG MS analyses described here exactly followed the procedures of a previous study [25]. Calculate the standard deviation of the electrical potential across all electrodes of the preprocessed EEG data as global field power (GFP) (formula (1), which is used to describe the intensity of the electric field of a topographic map.

$$GFP_i = \sqrt{\sum_i^N \left(x_i\left(t\right) - x_{mean}\left(t\right)\right)^2 \Big/ N} \tag{1}$$

where N is the number of electrodes, $x_i(t)$ represents the instantaneous potentials of electrode i at time t, and $x_{mean}(t)$

is the mean instantaneous potential of all electrodes at time t. Only the EEG topography at the peak (local maximum) of the GFP was subsequently analyzed, as the topography of the EEG map remained stable around the peak of the GFP. Modified K-means clustering was performed on the GFP-restricted data to identify the most dominant topographies as classes of MS. The algorithm was randomly initialized 30 times. Global explained variance as a measure of fit for microstate segmentation. The algorithm stops when the relative change in error between iterations drops below the threshold of 10^{-6} or the number of iterations reaches 1000. Clustering analysis was performed at the individual level in each group. Each group will obtain its own MS class model maps. Four MS classes have been reported in most studies to explain the variance in EEG data of healthy individuals and patients with psychotic disorders [7]. The resulting class-labeled group model maps were finally used as templates to assign individual model maps from each individual to four MS classes. The MS parameters, namely, duration, occurrence, coverage, and transition percentage, were calculated for the four MS classes in each group. Duration refers to the total time a given MS remains stable, which indicates the stability of subcortical neurons. Occurrence is the frequency of occurrence of a given MS class, which is thought to present a tendency for the nervous system to be activated. Coverage refers to the percentage of total record time for a given MS class. Transition percentage refers to the transition probabilities of a given MS class to any other MS class [14].

III. Microstate Brain Network Construction

In this section, the methods of construction, the properties, and the applications of the MS brain network are introduced separately. First, MS brain networks were constructed based on the dFC of intramicrostates and intermicrostates by the autoregressive (AR) model. Then, graph theory analysis was used to characterize the MS brain network topological metrics, indicating information integration and separation of the brain network. Finally, the correlation between the MS brain networks and disease pathological information was analyzed by the variance component model.

A. Dynamic Functional Connectivity

Brain networks of the EEG MSs were constructed from the intramicrostate FCs (intramsFCs) and intermicrostate FCs (intermsFCs) based on the same or different adjacent MS time series, respectively (Fig. 1). Specifically, according to the individual model map by MS analysis, each time point for an individual's entire time series was marked as MS class A (MS-A), MS-B, MS-C, or MS-D. Based on the different MSs, 6 different types of adjacent MS time series (i.e., MS-A&B, MS-A&C, MS-A&D, MS-B&C, MS-B&D, MS-C&D) and 4 kinds of adjacent MSs of the same type (i.e., MS-A&A, MS-B&B, MS-C&C, MS-D&D) were extracted. Combining these time series, a total of 10 new time series were obtained.

Previous studies evaluating dFC were primarily based on the entire original time series, but we defined two new types of MS FCs, including intramsFCs and intermsFCs, based on

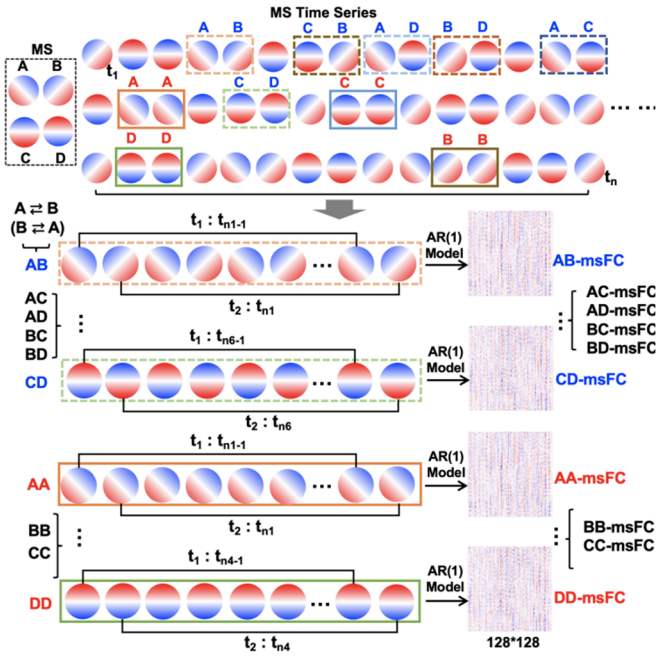

Fig. 1. The methodology assessing functional connections of intra- and intermicrostate dynamic functional connectivity (FC). A: microstate class A; B: microstate class B; C: microstate class C; D: microstate class D; msFC: FC of intra- or intermicrostates; AR(1): first-order autoregressive model. Four kinds of intramicrostate FCs: AA-msFC, BB-msFC, CC-msFC, and DD-msFC. Six kinds of intermicrostate FCs: AB-msFC, AC-msFC, AD-msFC, BC-msFC, BD-msFC, and CD-msFC.

the same or different types of MS time series. Typical dFC was also calculated as the comparison result of our algorithm.

MS network was established by the first-order AR (AR(1) model [26], [27], which is a dynamic measure of resting-state FC that is not limited by the classical sliding-window approach and can be used to explore the correlation of human behavior with resting-state brain function [28], as shown in formula (2):

$$\tilde{x}_t = W_t \cdot \tilde{x}_{t-1} + e_t \tag{2}$$

In formula (2), $\tilde{x}_t \in R^{N\times 1}$ represents the electrode vector at time point t in the newly composed time series; $W_t \in R^{N\times N}$ represents the parameter in the model that encodes the linear relationship between x_{t-1} and x_t; $e_t \in R^{N\times 1}$ represents an error vector at time t; and N is the number of electrodes. Formula (2) can be written as all-time points; each time point t has a W_t (except the first time point). A matrix was built to represent all the W_t values in a time series. Concatenating formula (2) at each time point yields the following matrix form:

$$\tilde{X}_{2:T} = \bar{W} \cdot \tilde{X}_{1:T-1} + E \tag{3}$$

In formula (3), $\tilde{X} \in R^{N\times T}$ represents the newly composed time-series matrix of electrodes; N is the number of electrodes; and T is the number of time points. $X_{2:T} \in R^{N\times T-1}$ represents the second column to the last column of X, and $X_{1:T-1} \in R^{N\times T-1}$ represents the first column to the penultimate column of X. $\bar{W} \in R^{N\times N}$ represents the comprehensive FC between nodes in the EEG time series, which is used for subsequent analysis. $E \in R^{N\times T-1}$ represents the error matrix in the model. $\bar{W}$ can be identified from the multivariate time series in formula (3) through the least squares method.

According to the types of MS classes, the 10 newly composed time series were input into formula (3). As a result, intramsFCs, including AA-msFC, BB-msFC, CC-msFC and DD-msFC, were generated. IntermsFCs, including AB-msFC, AC-msFC, AD-msFC, BC-msFC, BD-msFC, and CD-msFC, were generated. It is worth noting that we averaged the two alternate pairs, such as AB-msFC and BA-msFC, eventually resulting in only one type of msFC.

In addition, to verify that AR is a suitable method to construct FCs based on MS time series, we used the phase lag index (PLI) and Pearson correlation coefficient (PCC) for comparison. PCC measures the linear relationship between two random variables, which reflects the average functional organization of the entire neuroimaging recording. PLI measures the asymmetry in the distribution of the phase difference between two signals in the frequency domain [29], [30].

B. Graph Theoretical Analysis

Several network metrics based on graph theory, which has a special advantage in that it easily allows the formulation and evaluation of generative models, were calculated and analyzed here [31]. To characterize the features of three types of FC (intramsFCs, intermsFCs, and dFC), which were constructed based on the AR(1) model of formula (3), three main network (node) topological metrics were calculated using graph theory, which included global efficiency (E_{global}), local efficiency (E_{local}), and clustering coefficient (C_C). Considering that the three metrics can measure the communication efficiency of brain networks, among which E_{global} describes functional integration and E_{local} and C_C describe functional segregation [32], we can comprehensively characterize the information interaction in intramsFCs and intermsFCs from local and global perspectives.

First, a multiple thresholds approach was performed with the threshold being 0.1 to 0.4 and the step size being 0.01 on the 4 kinds of intramsFCs, 6 types of intermsFCs, and dFC. The threshold represents the percentage of the retained value based on the data in each matrix (e.g., 0.1 represents the maximum value of the first 10% of the data). It is worth noting that the multithreshold approach is more reliable than the specific threshold approach when examining schizophrenia and other psychiatric disorders [33]. Then, each type of FC generated 31 sparse matrices, which were put into formulas (4), (5), and (6).

$$E_{globali} = \frac{\sum_{j\in NS, j\neq i}\left(d_{ij}^{w}\right)^{-1}}{N-1} \tag{4}$$

$$E_{locali} = \frac{\sum_{j\in NS, j\neq i}\left(w_{ij}w_{ih}\left[d_{jh}^{w}\left(NS_i\right)\right]^{-1}\right)^{1/3}}{N-1} \tag{5}$$

$$C_{ci} = \frac{2t_i^w}{k_i\left(k_i-1\right)} \tag{6}$$

$$t_i^w = \frac{1}{2}\sum_{j,h\in NS}\left(w_{ij}w_{ih}w_{jh}\right)^{\frac{1}{3}} \tag{7}$$

For each sparse matrix, E_{global}, E_{local}, or C_C is the vector of $N \times 1$. NS is the set of all nodes in the network, and N is the number of nodes (electrodes). w_{ij} is the connection weight between node i and node j. d_{ij}^{w} is the shortest weighted path length between node i and node j. $d_{jh}^{w}(NS_i)$ is the length of the shortest path between node j and node h, which contains only neighbors of node i. Here, FC is directional. t_i^{w} is the weighted geometric mean of triangles around i, as shown in formula (7). k_i is the degree of node i. The final results were obtained by calculating the area under the curve (AUC) of the network topological metrics under each threshold [34].

The detailed calculation methods for C_C, E_{global}, and E_{local} were described in some previous literature [35]. The C_C is a measure of the degree to which nodes in a graph tend to cluster together and is considered a metric of network segregation. E_{global} is a scalar measure of information flow, which is used to measure the speed and efficiency of information transfer over the whole network to reflect the transfer capacity. E_{local} can be considered the average efficiency of local subgraphs.

C. Variance Component Model

To explore the physiological information contained in FCs (dFC, intramsFC, and intermsFC), we applied a multivariate variance component model to correlate network topological metrics with pathological information data. Network metrics were considered independent variables, and physiological information data were considered dependent variables.

The multivariate variance component model developed by Ge et al. [36] was used as shown in formula (8):

$$Y = E + U \tag{8}$$

where Y, E, or U is the matrix of $S \times H$. S is the number of individuals in each group, and H is the amount of pathological index information. Y is a multidimensional trait of S individuals. In this study, Y is the pathological index matrix. E and U represent common environmental factors and unique environmental factors, respectively, as shown in formulas (9)-(11):

$$F(i,j) = Corr(vec(TM_i), vec(TM_j)) \tag{9}$$

$$vec\,(E) \sim N(0, \Sigma_e \otimes F) \tag{10}$$

$$vec\,(U) \sim N(0, \Sigma_u \otimes I) \tag{11}$$

where $F(i, j)$ encodes the similarity of network topological metrics (E_{gobal}, E_{local}, or C_c) between individuals i and j. $Corr$ indicates the Pearson correlation analysis. $vec\,(.)$ is the matrix vectorization operator that converts a matrix into a vector by stacking its columns. $TM \in R^{N\times TF}$ is the topology metrics matrix of FCs, which is calculated by formulas (4), (5), or (6). N is the number of nodes. TF is the number of types of FCs; here, TF is the value of 6 (number of intermsFCs), 4 (number of intramsFCs) or 1 (number of dFCs). $\sim N()$ means that a vector is normally distributed. $\otimes$ is the Kronecker product of matrices. $F \in R^{S\times S}$ is a similarity matrix, which is generated by formula (9). I is an identity matrix, $\Sigma_e \in R^{H\times H}$ is a common environmental covariance matrix, and $\Sigma_u \in R^{H\times H}$ is the unique environmental covariance matrix, which is to be estimated from F and Y. The variance explained by network topological metrics of FC, denoted by M, was computed as shown in formula (12):

$$M = \frac{Tr(\Sigma_e)}{Tr\,(\Sigma_e) + Tr(\Sigma_u)} \tag{12}$$

where $Tr(.)$ is the trace operator, measuring the explanatory variance in the network topological metrics of msFC variability with the clinical performance of individuals. For each network topological metric (E_{global}, E_{local}, or C_c), 3 kinds of FCs are used, namely, inter-all-msFC, intra-all-msFC, and dFC, and three different Ms are calculated by formula (12). In the regression analysis of the multidimensional pathological index, the sex and age of individuals were used as basic covariates. Moreover, the parameters (durations, occurrences, and coverages) of four MS classes were used as additional covariates when analyzing the msFCs.

IV. Experiments and Results

For this section, we collected clinical data of patients with schizophrenia at different stages to verify the application of our proposed MS brain networks in revealing disease mechanisms and their advantages compared to traditional dynamic brain networks. First, individual resting-state EEG data and clinical scale information were collected, statistical analysis was performed, and the clinical performance (disease characteristics and cognitive function) of each group of individuals was quantified. The spatiotemporal characteristics of MSs and the differences in the topological metrics (E_{global}, E_{local}, and C_C) of the brain networks constructed by dFC and msFCs (intra and inter) were compared and analyzed. Finally, the degree of interpretation of clinical performance by the three types of brain networks was evaluated, which highlighted the value of MS brain networks in revealing underlying disease mechanisms.

A. Participant Recruitment

We applied the intra- and intermicrostate brain network methodology in the dataset obtained from 99 individuals, including 30 individuals with FES, 21 at UHR, 17 with familial HR, and 31 HC individuals. FES patients were diagnosed according to the Diagnostic and Statistical Manual of Mental Disorders, Fourth Edition (DSM-IV); UHR individuals were assessed by the Structured Interview of Psychosis-risk Syndrome (SIPS); unaffected first-degree relatives of individuals with schizophrenia who met DSM-IV diagnostic criteria served as HR individuals, and the HC group was recruited from the community. The clinical characteristics of individuals with FES were assessed based on the Positive and Negative Syndrome Scale (PANSS). The prodromal syndromes for the individuals of UHR, HR, and HC were assessed using SIPS. The exclusion criteria were education $<$ 6 years, significant intellectual disability (IQ $<$ 70), a history of head trauma, any psychiatric disorder, neurological disease, and substance abuse. All individuals were not using drugs, and therefore, the effects of antipsychotic drugs on cognitive outcomes were ruled out. This study was approved by the Science and Ethics Committee of the Beijing Anding Hospital of Capital Medical University by the Declaration of Helsinki, and all individuals provided informed consent. Kruskal–Wallis with post hoc tests were performed on the demographic data (sex, age, education and IQ) and clinical data (Calgary Depression Scale for Schizophrenia (CDSS) and SIPS), and significance values were adjusted by the Bonferroni correction for multiple tests ($p < 0.05$). Demographic and clinical details are summarized in Supplemental Table 1.

B. Dataset Construction

For the four groups of individuals recruited, resting-state EEG data collection was contained in dataset 1, and cognitive function assessments by the Measurement and Treatment Research to Improve Cognition in Schizophrenia (MATRICS) Consensus Cognitive Battery (MCCB) and clinical characteristics based on PANSS for those with schizophrenia were contained in dataset 2.

Dataset 1: Resting-state EEG data. The EEG was recorded for each individual in the four groups from a 128-scalp electrode (Electrical Geodesic Inc., EGI, Eugene, OR) attached to the entire scalp by the international 10-20 system at 1000 Hz, and a reference electrode was Cz. The EEG acquisition impedance was kept below 5 kΩ. All individuals recorded three minutes of resting-state data with eyes closed. EEG data preprocessing was performed, and artifact rejection methods were implemented utilizing algorithms in the MATLAB (Version 2017a, The MathWorks, Natick, MA, United States) toolbox EEGLab [37]. Independent component analysis was used to identify and remove the artifacts from raw EEG signals. Artifact-free EEG data were downsampled to 128 Hz and bandpass filtered from 1-40 Hz using a basic finite impulse response filter [9].

Dataset 2: Physiological index information (MCCB and PANSS). The neurocognitive domain performance of all the individuals was assessed by the MCCB, which is a standardized battery for patients with schizophrenia and related disorders [38]. The MCCB includes nine standardized neurophysiologic tests that reflect seven cognitive domains. Specifically, speed of processing (*Brief Assessment of Cognition in Schizophrenia*-Symbol Coding, *Category Fluency*-Animal Naming, and *Trail Making Test-Part A*), attention/vigilance (*Continuous Performance Test*), working memory (*Wechsler Memory Scale-Spatial Span*), verbal learning (*Hopkin's Verbal Learning Test-Revised*), visual learning (*Brief Visuospatial Memory Test-Revised*), reasoning and problem-solving (*Neuropsychological Assessment Battery-Mazes*), and social cognition (*Mayer-Salovey-Caruso Emotional Intelligence Test-Managing Emotions*) [5]. The PANSS is a rating scale that helps researchers and clinicians measure the severity of psychiatric symptoms in patients with schizophrenia (FES group).

C. Cognitive Performance

One-way ANOVA or Kruskal-Wallis with post hoc tests were performed on MCCB scores in each group (Fig. 2). The results of the statistical analyses between groups showed that the four groups had significant differences in the following cognitive abilities: speed of processing ($F = 9.947$, $p < 0.001$), attention/vigilance ($F = 15.289$, $p < 0.001$), working memory ($H = 15.185$, $p = 0.002$), verbal learning ($H = 14.086$, $p = 0.003$), social cognition ($F = 3.039$, $p = 0.033$) and MCCB total score ($H = 26.041$, $p < 0.001$); however, there were no significant differences in visual learning ($H = 4.683$, $p > 0.05$) or reasoning and problem learning ($H = 3.362$, $p > 0.05$). Cognitive performance in the FES group displayed the

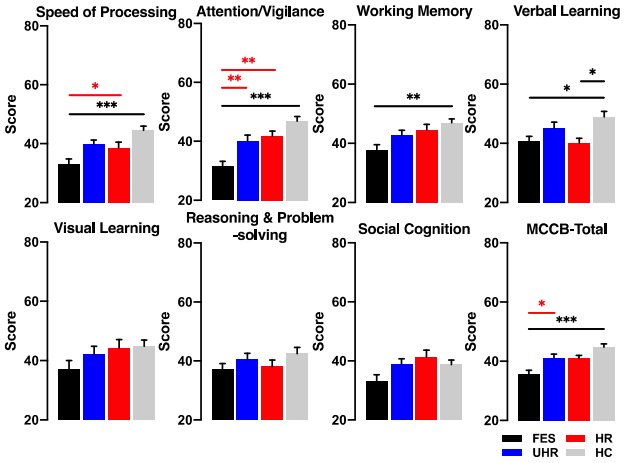

Fig. 2. Cognitive test performance in the four groups (FES, UHR, HR, and HC) was evaluated by the MCCB test. Bar graphs display the mean (standard error) scores on the MCCB test. Comparisons with the HC group are indicated by black lines, and comparisons with the FES group are indicated by red lines. * $p < 0.05$, ** $p < 0.01$, *** $p < 0.001$. All p values are corrected with Bonferroni correction.

lowest score among the four groups, especially for the speed of processing, attention/vigilance, working memory, verbal learning, social cognition (FES vs HR, $p = 0.05$) and total score on the MCCB. The post hoc test results are shown in detail in Supplemental Table 2.

D. Microstate Spatiotemporal Characteristics

Grand mean model MS maps for the four groups (FES, UHR, HR, and HC) are displayed in Fig. 3A. The extracted MSs closely resembled the canonical four MS classes A to D. For each individual in the four groups, three parameters per MS class were computed: time coverage, mean duration, and frequency of occurrence. Group average statistics are depicted in Fig. 3B. One-way ANOVA or Kruskal–Wallis with post hoc tests were performed on MS parameters. The predominant differences in parameters among the four groups were in MS-A (group effects: coverage: $H = 17.400$, $p = 0.001$; duration: $H = 11.889$, $p = 0.008$; occurrence: $H = 18.149$, $p < 0.001$) and MS-C (coverage: $F = 3.507$, $p = 0.018$; duration: $H = 12.126$, $p = 0.007$). There were no significant differences across groups in MS-B and MS-D ($p > 0.05$).

Compared to the HC group, the FES group showed significantly decreased time coverage ($p = 0.001$), slower occurrence ($p < 0.05$) and shorter duration ($p = 0.015$) in MS-A and increased time coverage ($p = 0.025$) and longer duration ($p = 0.018$) in MS-C. The UHR and exhibited significantly lower coverage ($p = 0.028$) and slower occurrence ($p = 0.028$) in MS-A. And the HR groups showed significantly lower coverage ($p = 0.034$) and duration ($p = 0.047$) in MS-A.

E. Network Topological Metrics

Here, 6 kinds of intermsFCs (i.e., between two different MSs) and 4 kinds of intramsFCs (i.e., within two identical MSs) based on the AR(1) model were constructed. As a comparison, typical FCs based on the entire time series (dFCs) were built for four groups. The results in Fig. 4 display the group differences in the network topological metrics, i.e., E_{global}, E_{local}, and C_C, of dFCs and msFCs (inter and intra). The detailed statistical analysis results of Kruskal–Wallis and

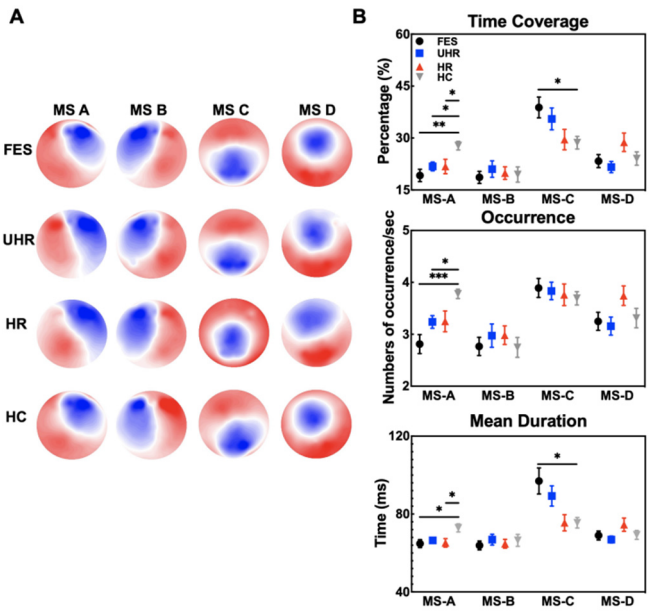

Fig. 3. The spatial configuration of microstate classes A-D and microstate parameters. EEG topo plots showing microstate topographies derived from quiet rest EEG recordings in the four groups (FES, UHR, HR, and HC) (A). Although red is positive and blue is negative, microstate analysis ignores polarity. Dot plots display the mean (standard error) of the time coverage, occurrence, and duration in the four groups (B). Comparisons with the HC group are indicated by black lines. * $p < 0.05$, ** $p < 0.01$, *** $p < 0.001$. All p values are corrected with Bonferroni correction.

post hoc tests across groups in network topological metrics are shown in Supplemental Table 3. In the FES and UHR groups, significant reductions in E_{global} were observed in all intramsFCs and some intermsFCs. For the HR group, only the E_{global} values of intramsFCs (AAmsFCs) were significantly higher than those in the UHR group (Fig. 4A). There was no significant difference across groups in E_{local} of msFCs (intra and inter) in the four groups (Fig. 4B). For the individuals in the FES and UHR groups, the C_C values of msFCs (intra and inter) were significantly higher than those in the HC group (Fig. 4C). However, there was no significant difference in dFC (E_{global}, E_{local}, or C_C) among the four groups.

F. Brain Network Encoding Clinical Performance

To further explore the impact of functional network topological metrics on clinical performance, the correlations between E_{global}, E_{lobal}, and C_c with MCCB and PANSS total scores were computed (Fig. 5). We used the delete-1 jackknife approach to evaluate significant differences between the variance explained by three different methods of FCs (intermsFC, intramsFC, and dFC). Specifically, the M derived from inter- and intramsFCs and dFC were compared. During the period, subject i was randomly removed from each set of data, M_i was calculated with the above formula (12), S values of M were generated by looping S times, and then one-way ANOVA was used for comparison.

The results in Fig. 5A show that the cognitive performance of the healthy subjects was better explained by E_{global} of dFC than that of all-msFC subjects (intermsFC and intramsFC). However, for the patient groups (FES, UHR, and HR), the h^2 values of E_{global} were contrary to those of the HC group, and cognitive performance was better explained by

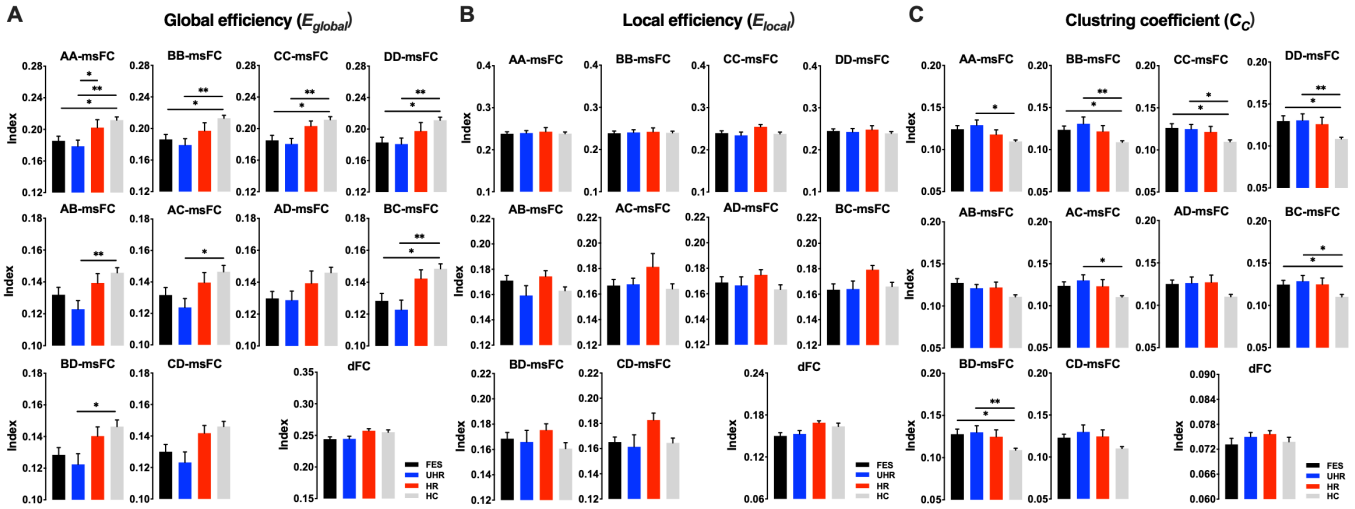

Fig. 4. Group differences in network topological metrics of msFCs and dFCs across the four groups. Bar graphs display the mean (standard error) of the E_{global} (A), E_{local} (B), and C_C (C) indices in the four groups (FES, UHR, HR and HC). Compared with the HC group, * $p < 0.05$, ** $p < 0.01$. All p values are corrected with Scheffe correction. Four kinds of intramsFCs: AA-msFC, BB-msFC, CC-msFC, and DD-msFC. Six kinds of intermsFCs: AB-msFC, AC-msFC, AD-msFC, BC-msFC, BD-msFC, and CD-msFC.

inter-all-msFCs and intra-all-msFCs. Regarding E_{local} and C_C(Fig. 5B-C), all-msFCs contributed a higher association with cognitive performance; specifically, intermsFCs showed the highest association among the three kinds of FCs in the four groups. In addition, PANSS total scores in the FES group were better explained by E_{global} of inter all-msFCs, which showed the highest h^2 -value among the three kinds of FCs (Fig. 5D). The detailed statistical analysis results are shown in Supplemental Tables 4 and 5.

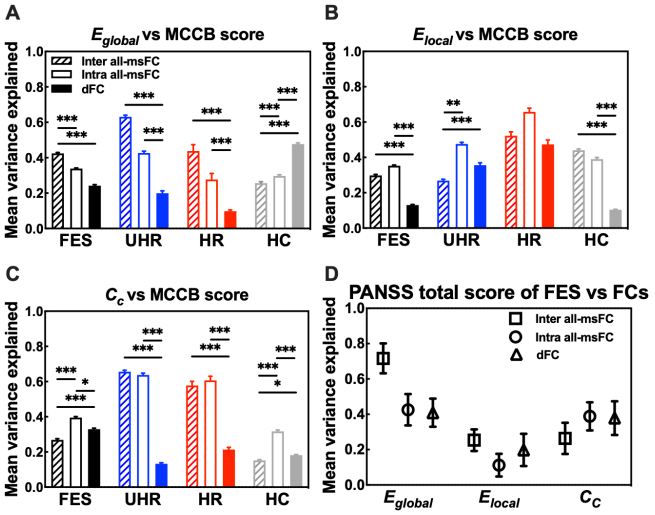

Fig. 5. The explain ability of network topology metrics for clinical presentation. One -way ANOVA is used to compare the variance explained (h^2 value) of different types of FC in same group. Bar graphs display the mean (standard error) of variance explained (h^2 value) between the E_{global}, E_{lobal}, and C_C of dFCs and all-msFCs (inter and intra) with MCCB scores in four groups (FES, UHR, HR, and HC) (A-C). * $p < 0.05$, ** $p < 0.01$, *** $p < 0.001$. All p values are corrected with Bonferroni correction. Box graphs display the mean (standard deviation) of the h^2 value between the dFCs and all-msFCs (inter and intra) with PANSS total scores (D).

V. Discussion

EEG MSs have been shown to reflect many cognitive processes and to be associated with the pathology of schizophrenia. FC analysis of resting neural activity (such as blood oxygen level-dependent signals, EEG data, etc.) can characterize the nature of interactions of brain networks and help reveal brain activity patterns. In this study, we aimed to explore the differences in the dynamic brain networks of EEG MSs in the different stages of schizophrenia and the impact on individuals' cognitive deficits. Finally, we confirmed the cognitive status and MS characteristics of the four groups (FES, UHR, HR, and HC), constructed intra- and intermicrostate networks and finally explored the relationship between MS network topological metrics and cognitive deficits in individuals with schizophrenia and those in a high-risk state.

A. Clinical Symptoms and Cognitive Deficits

Here, we administered clinical assessments and cognitive tests in four groups of individuals, namely, those with FES, UHR, HR, and HC, using the CDSS, SIPS, PANSS, and MCCB. The evaluation of depression level by the CDSS showed that compared with the HC group, the three other groups (FES, UHR, and HR) exhibited significantly more depressive symptoms. Notably, the UHR group had the highest CDSS scores. The SIPS was used to assess the prodromal stages of schizophrenia, and our results showed that the clinical symptoms gradually increased as schizophrenia progressed (UHR > HR), which showed that the score increased compared with the HC group. The FES group was assessed for clinical symptoms by the PANSS, and the total PANSS score (mean = 85.23, SD = 12.52) was considered "moderately ill", which was higher than a PANSS score of 75 [39] (Supplemental Table 1). In addition, we investigated the cognitive deficits evaluated with the MCCB in the four groups. Consistent with previous studies, cognitive deficits are the central feature of schizophrenia, and individuals in a high-risk state exhibit cognitive deficits as commonly as those with schizophrenia [5], [40]. Fig. 2 shows that the FES group had the most serious cognitive deficits, especially for speed of processing, attention/vigilance, working memory and verbal learning (FES vs HC: $p < 0.05$). And the UHR or HR group was significantly different from the FES group in speed

of processing or attention/vigilance ($p < 0.05$). Our findings suggest that in addition to clinical symptoms, cognitive deficits gradually become more severe as the individual progresses through stages of schizophrenia.

B. Importance of MS-A and MS-C

The majority of studies have reported that the EEG MSs measured in patients with schizophrenia had abnormal time dynamics compared with controls. However, it is worth investigating the EEG MSs in schizophrenia stages I, II, and III at the same time to provide potential biomarkers for early diagnosis and intervention. Here, we divided the MSs observed in the four groups (FES, UHR, HR, and HC) into four classes, A, B, C, and D, in which the optimal number of MS classes depends on the dataset analyzed and previous work (Fig. 3). A meta-analysis revealed that patients with schizophrenia have a higher frequency and longer duration of MS-C and a lower frequency and shorter duration of MS-D than controls [41]. In addition, previous studies have shown that high-risk individuals displayed more coverage and occurrence of MS-A than first-episode patients with schizophrenia [12], and patients with early-course psychosis had a decreased frequency of MS-A [20]. Several studies combining simultaneous fMRI and EEG recordings have demonstrated that MS-A is related to auditory networks, and MS-C is related to the salience network [17]; interestingly, patients with recent-onset schizophrenia have decreased FC in the auditory networks compared to HCs [42]. Furthermore, aberrant FC in the default mode and salience networks correlates with psychotic symptoms in schizophrenia [43], [44], [45]. The patients with schizophrenia and individuals in the high-risk state showed similar abnormalities in EEG MSs. Consistent with some previous studies, our results showed that FES individuals exhibited significantly decreased time coverage, occurrence, and duration in MS-A and significantly increased time coverage and duration in MS-C compared with HCs. Regarding the UHR and HR groups, the results showed that only MS-A patients displayed significant differences compared with the HC group. Some studies have found that adolescents with 22q11.2 deletion syndrome with elevated MS-C have a 30% risk of developing schizophrenia. Moreover, MS-C and MS-D of EEG are considered candidate endophenotypes for schizophrenia, and more MS-C and less MS-D were shown in schizophrenia patients and their siblings [9]. It was found in our results that the duration in MS-C of the HR group ($p = 0.056$ with corrected) was marginally significant compared with the FES group. Therefore, we support MS-C as a potential biomarker for conversion to schizophrenia. Our results mainly suggest that MS-A plays a key role in schizophrenia and high-risk stages.

C. Disrupted Organization of msFCs

Previous results on disrupted functional brain networks in schizophrenia have been inconsistent. Several possible reasons might have caused these discrepancies. The variations in methods used to define FC play a key role. The present study is the first to explore dynamic information interactions from the view of intra- and intermicrostates of EEG in different stages of schizophrenia. We constructed dynamic brain networks for 6 kinds of intermicrostates and 4 kinds of intramicrostates in four groups (FES, UHR, HR, and HC) using the AR(1) model (Fig. 1), which was motivated by accounting for the memory present (i.e., X_t depends on X_{t-1}) in the MS time series [27]. The dynamic model considers the known biophysical properties of the neuron population in simulating the dynamics of brain function, and it is better for shaping resting-state brain function to characterize the dynamic connection [46], [47]. Furthermore, we constructed brain networks based on the PLI and PCC methods, and the results of topological metrics showed that there were no significant group effects in the brain network based on PLI, and the PCC network only exhibited a significant difference in C_C (Supplemental Table 6). However, AR network topological metrics have significant group effects, which is more conducive to capturing the pathological features in the intermsFCs or intramsFCs. Our E_{global} results showed that there was a predominant decrease in FCs in the patients, which suggested that the speed and efficiency of information integration decreased. With the progression of the disease, there was gradual destruction from the intramicrostate networks to the intermicrostate networks. In contrast, the results with the C_C values exhibited a significant increase in msFCs (intra and inter) in the patients compared with the HC group, which reflected the increase in segregation and greater templating of the network (Fig. 4). Our results are consistent with some previous studies evaluating EEG or fMRI functional networks [48]. Network studies of graph theory have revealed longer average path lengths and corresponding reductions in global communication efficiency, indicating decreased communication between more segregated parts of the brain in schizophrenia patients [49], [50]. Structural studies have found increased segregation (i.e., clustering) and reduced integration in patients with psychosis (i.e., lower E_{global}) [51]. Empirical findings have shown that patients with schizophrenia show a lower clustering in cognitive tasks and a higher clustering in the baseline period when a larger integration of cortical activity among distant brain regions is needed [52]. Whole-brain studies of FC changes have shown widespread reductions during rest in chronic patients [53]. Furthermore, in the present study, dFC failed to discriminate differences in brain networks between patients and healthy individuals ($p > 0.05$). We tried to detect patients by support vector machine using the metric of msFC and evaluated the area under the curve values to evaluate the classification effect. And the results in Supplemental Table 7 show that compared with previously constructed classification models for patients with schizophrenia in different stages based on EEG features [54] and even microstate features [15], [55], [18], the msFC-based classification model can achieve better performance in distinguishing FES, UHR, or HR with HC (AUC: 92.50%, 97.22%, or 88.63%) (Supplemental Table 8). It seems that the msFCs of MSs might be better at exhibiting changes during the progression of the disease. Above all, our findings suggest that there was a gradually disrupted organization of intramsFCs to intermsFCs as the stage of schizophrenia increased, resulting

in new insights revealing abnormal connectivity of MSs in neurodevelopmental disorders.

D. Effects of msFCs on Cognitive Deficits

Variations in brain network organization are robustly associated with individual differences in cognitive function [56]. In this study, we attempted to explore how the msFCs of MSs relate to cognitive deficits and performance in individuals with FES, UHR, and HR and HCs. The results showed that E_{global} of intermicrostate networks and E_{local}, C_C of intramicrostate networks encode more regarding cognitive performance (i.e., MCCB scores) than a common dFC metric in patients (FES, UHR, and HR). These results might suggest that the integration of information of intermicrostate networks and segregation of the intramicrostate networks well explain cognitive performance in patients. However, the E_{global} results in the HC group were exactly the opposite of those in the patients, in which the correlation between FC and MCCB scores ranked as dFC > intramsFC > intermsFC (Fig. 5). E_{local} and C_C msFCs showed higher associations than dFC, which was similar to those in the patient groups (FES, UHR, and HR). In addition, the E_{global} of FCs might play a core role in patients with cognitive deficits compared to HC individuals, which supports the notion, based on conceptual studies, that abnormal connectivity and disruption of information integration may be core aspects of the disease [57], [58]. Furthermore, our results showed that E_{global} in FES individuals contributed the most to the association between a functional network of intermicrostates and clinical symptoms (i.e., PANSS total scores), which supports the notion that FC alterations might also capture stable or intrinsic components of disease pathophysiology [59]. Therefore, our findings argue that the decrease in the integration of information intermicrostate networks might have a crucial role in the cognitive deficits of patients in different stages of schizophrenia.

E. Limitations and Future Work

Considering the lack of knowledge regarding "real" functional networks to provide the gold standard for evaluation of these results, it is inappropriate to be too confident about which FC construction algorithm is best. The AR(1) model was used for the first time to explore EEG MS networks. Although we used two other traditional methods (PLI and PCC) for constructing brain networks for comparison, and previous studies have shown that the behavioral information with AR(1)-based FC dynamic coding in MRI is significantly more than the common static FC index, it is essential to evaluate the stability of the algorithm using public datasets. Nighty-nine individuals who included those with FES, UHR, HR, and HC were recruited in this study, which is the largest number of subjects in the current study to simultaneously include different schizophrenia disease stages to our knowledge, increasing the sample size and balancing the number of groups will be one of the effective methods to further verify the reliability of model. In addition, cognitive integration in resting-state FC has been shown to encode, self-reports have lower requirements for information integration compared with complex cognitive tasks. Many studies have shown that there are differences in the network characteristics of cognitive processing in patients with schizophrenia. Exploring the intra- and intermicrostate networks in the context of cognitive task performance might be better for revealing differences in the changes in FC dynamics and supplementing our current understanding of the neural mechanisms underlying cognitive deficits in different stages of schizophrenia.

VI. Conclusion

The results presented in this paper yield new insights into the dynamic changes in brain networks in different stages of schizophrenia. In addition to explaining the importance of the parameters of MS classes A and C in the progression of the disease, our results provide a new perspective regarding EEG MSs from information interactions. Our findings suggest that disrupted organization of brain networks from intramicrostates to intermicrostates with disease progression and decreased integration of information intermicrostates might lead to cognitive deficits in schizophrenia and individuals in high-risk states. This work contributes to the characterization of dynamic functional brain networks based on EEG signals from a new perspective and provides a new interpretation of pathological brains, especially for schizophrenia.

References

[1] R. S. Kahn et al., "Schizophrenia," *Nature Rev. Disease Primers*, vol. 1, no. 1, p. 15067, Nov. 2015.
[2] Y. Luo et al., "Discriminating schizophrenia disease progression using a P50 sensory gating task with dense-array EEG, clinical assessments, and cognitive tests," *Expert Rev. Neurotherapeutics*, vol. 19, no. 5, pp. 459–470, May 2019.
[3] Y.-M. Wang et al., "Altered brain structural and functional connectivity in schizotypy," *Psychol. Med.*, vol. 2020, pp. 1–10, Jul. 2020.
[4] Y. Li, M. Chen, S. Sun, and Z. Huang, "Exploring differences for motor imagery using Teager energy operator-based EEG microstate analyses," *J. Integrative Neurosci.*, vol. 20, no. 2, pp. 411–417, Jun. 2021.
[5] Y. Luo, Q. Tian, C. Wang, K. Zhang, C. Wang, and J. Zhang, "Biomarkers for prediction of schizophrenia: Insights from resting-state EEG microstates," *IEEE Access*, vol. 8, pp. 213078–213093, 2020.
[6] J. Kindler, D. Hubl, W. K. Strik, T. Dierks, and T. Koenig, "Resting-state EEG in schizophrenia: Auditory verbal hallucinations are related to shortening of specific microstates," *Clin. Neurophysiol.*, vol. 122, no. 6, pp. 1179–1182, Jun. 2011.
[7] B. A. Seitzman, M. Abell, S. C. Bartley, M. A. Erickson, A. R. Bolbecker, and W. P. Hetrick, "Cognitive manipulation of brain electric microstates," *NeuroImage*, vol. 146, pp. 533–543, Feb. 2017.
[8] S. Soni, S. P. Muthukrishnan, M. Sood, S. Kaur, and R. Sharma, "Hyperactivation of left inferior parietal lobule and left temporal gyri shortens resting EEG microstate in schizophrenia," *Schizophrenia Res.*, vol. 201, pp. 204–207, Nov. 2018.
[9] J. R. da Cruz et al., "EEG microstates are a candidate endophenotype for schizophrenia," *Nature Commun.*, vol. 11, no. 1, pp. 1–10, Jun. 2020.
[10] R. de Bock, A. J. Mackintosh, F. Maier, S. Borgwardt, A. Riecher-Rössler, and C. Andreou, "EEG microstates as biomarker for psychosis in ultra-high-risk patients," *Transl. Psychiatry*, vol. 10, no. 1, pp. 1–6, Aug. 2020.
[11] K.-K. Chen et al., "Efficacy of short-term multidisciplinary intensive rehabilitation in patients with different Parkinson's disease motor subtypes: A prospective pilot study with 3-month follow-up," *Neural Regener. Res.*, vol. 16, no. 7, pp. 1336–1343, Jul. 2021.
[12] C. Andreou et al., "Resting-state connectivity in the prodromal phase of schizophrenia: Insights from EEG microstates," *Schizophrenia Res.*, vol. 152, nos. 2–3, pp. 513–520, Feb. 2014.
[13] K. Nishida et al., "EEG microstates associated with salience and frontoparietal networks in frontotemporal dementia, schizophrenia and Alzheimer's disease," *Clin. Neurophysiol.*, vol. 124, no. 6, pp. 1106–1114, Jun. 2013.

[14] D. Lehmann et al., "EEG microstate duration and syntax in acute, medication-naïve, first-episode schizophrenia: A multi-center study," *Psychiatry Res., Neuroimaging*, vol. 138, no. 2, pp. 141–156, Feb. 2005.

[15] K. Kim, N. T. Duc, M. Choi, and B. Lee, "EEG microstate features for schizophrenia classification," *PLoS ONE*, vol. 16, no. 5, May 2021, Art. no. e0251842.

[16] A. Khanna, A. Pascual-Leone, C. M. Michel, and F. Farzan, "Microstates in resting-state EEG: Current status and future directions," *Neurosci. Biobehav. Rev.*, vol. 49, pp. 105–113, Feb. 2015.

[17] C. M. Michel and T. Koenig, "EEG microstates as a tool for studying the temporal dynamics of whole-brain neuronal networks: A review," *NeuroImage*, vol. 180, pp. 577–593, Oct. 2018.

[18] M. Baradits, I. Bitter, and P. Czobor, "Multivariate patterns of EEG microstate parameters and their role in the discrimination of patients with schizophrenia from healthy controls," *Psychiatry Res.*, vol. 288, Jun. 2020, Art. no. 112938.

[19] A. Mishra, B. Englitz, and M. X. Cohen, "EEG microstates as a continuous phenomenon," *NeuroImage*, vol. 208, Mar. 2020, Art. no. 116454.

[20] M. Murphy, R. Stickgold, and D. Öngür, "Electroencephalogram microstate abnormalities in early-course psychosis," *Biol. Psychiatry, Cognit. Neurosci. Neuroimaging*, vol. 5, no. 1, pp. 35–44, Jan. 2020.

[21] J. Britz, D. Van De Ville, and C. M. Michel, "BOLD correlates of EEG topography reveal rapid resting-state network dynamics," *NeuroImage*, vol. 52, no. 4, pp. 1162–1170, Oct. 2010.

[22] R. Yao et al., "Dynamic changes of brain networks during working memory tasks in schizophrenia," *Neuroscience*, vol. 453, pp. 187–205, Jan. 2021.

[23] A. Kaur, V. Chinnadurai, and R. Chaujar, "Microstates-based resting frontal alpha asymmetry approach for understanding affect and approach/withdrawal behavior," *Sci. Rep.*, vol. 10, no. 1, pp. 1–22, Mar. 2020.

[24] C. V. Latchoumane, I. Kim, H. Sohn, and J. Jeong, "Dynamical nonstationarity of resting EEGs in patients with attention-deficit/hyperactivity disorder (AD/HD)," *IEEE Trans. Biomed. Eng.*, vol. 60, no. 1, pp. 159–163, Jan. 2013.

[25] T. Koenig, D. Lehmann, M. C. G. Merlo, K. Kochi, D. Hell, and M. Koukkou, "A deviant EEG brain microstate in acute, neuroleptic-naive schizophrenics at rest," *Eur. Arch. Psychiatry Clin. Neurosci.*, vol. 249, no. 4, pp. 205–211, Aug. 1999.

[26] P. A. Valdés-Sosa et al., "Estimating brain functional connectivity with sparse multivariate autoregression," *Phil. Trans. Roy. Soc. B, Biol. Sci.*, vol. 360, no. 1457, pp. 969–981, May 2005.

[27] R. Liégeois, T. O. Laumann, A. Z. Snyder, J. Zhou, and B. T. T. Yeo, "Interpreting temporal fluctuations in resting-state functional connectivity MRI," *NeuroImage*, vol. 163, pp. 437–455, Dec. 2017.

[28] R. Liégeois et al., "Resting brain dynamics at different timescales capture distinct aspects of human behavior," *Nature Commun.*, vol. 10, no. 1, p. 2317, May 2019.

[29] C. J. Stam, G. Nolte, and A. Daffertshofer, "Phase lag index: Assessment of functional connectivity from multi channel EEG and MEG with diminished bias from common sources," *Hum. Brain Mapping*, vol. 28, no. 11, pp. 1178–1193, Nov. 2007.

[30] A. M. Bastos and J.-M. Schoffelen, "A tutorial review of functional connectivity analysis methods and their interpretational pitfalls," *Frontiers Syst. Neurosci.*, vol. 9, p. 175, Jan. 2016.

[31] Q. Yu et al., "Assessing dynamic brain graphs of time-varying connectivity in fMRI data: Application to healthy controls and patients with schizophrenia," *NeuroImage*, vol. 107, pp. 345–355, Feb. 2015.

[32] M. Rubinov and O. Sporns, "Complex network measures of brain connectivity: Uses and interpretations," *NeuroImage*, vol. 52, no. 3, pp. 1059–1069, Sep. 2010.

[33] M. P. van den Heuvel, S. C. de Lange, A. Zalesky, C. Seguin, B. T. T. Yeo, and R. Schmidt, "Proportional thresholding in resting-state fMRI functional connectivity networks and consequences for patient-control connectome studies: Issues and recommendations," *NeuroImage*, vol. 152, pp. 437–449, May 2017.

[34] S. M. H. Hosseini, F. Hoeft, and S. R. Kesler, "GAT: A graph-theoretical analysis toolbox for analyzing between-group differences in large-scale structural and functional brain networks," *PLoS ONE*, vol. 7, no. 7, Jul. 2012, Art. no. e40709.

[35] M. Rubinov and O. Sporns, "Complex network measures of brain connectivity: Uses and interpretations," *NeuroImage*, vol. 52, no. 3, pp. 1059–1069, Sep. 2010.

[36] T. Ge et al., "Multidimensional heritability analysis of neuroanatomical shape," *Nature Commun.*, vol. 7, no. 1, p. 13291, Nov. 2016.

[37] A. Delorme and S. Makeig, "EEGLAB: An open source toolbox for analysis of single-trial EEG dynamics including independent component analysis," *J. Neurosci. Methods*, vol. 134, no. 1, pp. 9–21, Mar. 2004.

[38] C. Shi et al., "The MATRICS consensus cognitive battery (MCCB): Co-norming and standardization in China," *Schizophrenia Res.*, vol. 169, nos. 1–3, pp. 109–115, Dec. 2015.

[39] S. Leucht, J. Kane, W. Kissling, J. Hamann, E. Etschel, and R. Engel, "What does the PANSS mean?" *Schizophrenia Res.*, vol. 79, nos. 2–3, pp. 231–238, Nov. 2005.

[40] A. Üçok et al., "Cognitive deficits in clinical and familial high risk groups for psychosis are common as in first episode schizophrenia," *Schizophrenia Res.*, vol. 151, nos. 1–3, pp. 265–269, Dec. 2013.

[41] K. Rieger, L. Diaz Hernandez, A. Baenninger, and T. Koenig, "15 years of microstate research in schizophrenia—Where are we? A meta-analysis," *Frontiers Psychiatry*, vol. 7, p. 22, Feb. 2016.

[42] S. W. Joo, W. Yoon, Y. T. Jo, H. Kim, Y. Kim, and J. Lee, "Aberrant executive control and auditory networks in recent-onset schizophrenia," *Neuropsychiatric Disease Treat.*, vol. 16, pp. 1561–1570, 2020, 2020.

[43] J. Lefort-Besnard et al., "Different shades of default mode disturbance in schizophrenia: Subnodal covariance estimation in structure and function," *Hum. Brain Mapping*, vol. 39, no. 2, pp. 644–661, Feb. 2018.

[44] H. Littow et al., "Aberrant functional connectivity in the default mode and central executive networks in subjects with schizophrenia—A whole-brain resting-state ICA study," *Frontiers Psychiatry*, vol. 6, p. 110, Feb. 2015.

[45] A. Rotarska-Jagiela, V. van de Ven, V. Oertel-Knöchel, P. J. Uhlhaas, K. Vogeley, and D. E. J. Linden, "Resting-state functional network correlates of psychotic symptoms in schizophrenia," *Schizophrenia Res.*, vol. 117, no. 1, pp. 21–30, Mar. 2010.

[46] M. Breakspear, V. Jirsa, and G. Deco, "Computational models of the brain: From structure to function," *NeuroImage*, vol. 52, no. 3, pp. 727–730, Sep. 2010.

[47] J. Casorso, X. Kong, W. Chi, D. Van De Ville, B. T. T. Yeo, and R. Liégeois, "Dynamic mode decomposition of resting-state and task fMRI," *NeuroImage*, vol. 194, pp. 42–54, Jul. 2019.

[48] J. A. Hadley, N. V. Kraguljac, D. M. White, L. Ver Hoef, J. Tabora, and A. C. Lahti, "Change in brain network topology as a function of treatment response in schizophrenia: A longitudinal resting-state fMRI study using graph theory," *NPJ Schizophrenia*, vol. 2, no. 1, p. 16014, Apr. 2016.

[49] M. P. Van Den Heuvel and A. Fornito, "Brain networks in schizophrenia," *Neuropsychol. Rev.*, vol. 24, no. 1, pp. 32–48, 2014.

[50] M.-C. Ottet, M. Schaer, M. Debbané, L. Cammoun, J.-P. Thiran, and S. Eliez, "Graph theory reveals dysconnected hubs in 22q11DS and altered nodal efficiency in patients with hallucinations," *Frontiers Hum. Neurosci.*, vol. 7, Sep. 2013.

[51] M. P. van den Heuvel and R. S. Kahn, "Abnormal brain wiring as a pathogenetic mechanism in schizophrenia," *Biol. Psychiatry*, vol. 70, no. 12, pp. 1107–1108, Dec. 2011.

[52] J. Gomez-Pilar et al., "Functional EEG network analysis in schizophrenia: Evidence of larger segregation and deficit of modulation," *Prog. Neuro-Psychopharmacol. Biol. Psychiatry*, vol. 76, pp. 116–123, Jun. 2017.

[53] A. Zalesky, A. Fornito, and E. T. Bullmore, "Network-based statistic: Identifying differences in brain networks," *NeuroImage*, vol. 53, no. 4, pp. 1197–1207, Dec. 2010.

[54] S. Tikka et al., "Artificial intelligence-based classification of schizophrenia: A high density electroencephalographic and support vector machine study," *Indian J. Psychiatry*, vol. 62, no. 3, p. 273, 2020.

[55] E. Lillo, M. Mora, and B. Lucero, "Automated diagnosis of schizophrenia using EEG microstates and deep convolutional neural network," *Expert Syst. Appl.*, vol. 209, Dec. 2022, Art. no. 118236.

[56] A. Zalesky et al., "Whole-brain anatomical networks: Does the choice of nodes matter?" *NeuroImage*, vol. 50, no. 3, pp. 970–983, Apr. 2010.

[57] M. E. Lynall et al., "Functional connectivity and brain networks in schizophrenia," *J. Neurosci.*, vol. 30, no. 28, pp. 9477–9487, Jul. 14, 2010.

[58] M. P. van den Heuvel and O. Sporns, "Network hubs in the human brain," *Trends Cognit. Sci.*, vol. 17, no. 12, pp. 683–696, Dec. 2013.

[59] G. Collin, R. S. Kahn, M. A. de Reus, W. Cahn, and M. P. van den Heuvel, "Impaired rich club connectivity in unaffected siblings of schizophrenia patients," *Schizophr Bull.*, vol. 40, no. 2, pp. 438–448, Mar. 2014.